A Posteriori Error Estimates Based on the Polynomial Preserving Recovery

Ahmed Naga and Zhimin Zhang*
Department of Mathematics, Wayne State University

Abstract Superconvergence of order $O(h^{1+\rho})$, for some $\rho > 0$, is established for the gradient recovered with the Polynomial Preserving Recovery (PPR) when the mesh is mildly structured. Consequently, the PPR-recovered gradient can be used in building an asymptotically exact *a posteriori* error estimator.

Key Words. finite element method, the SPR, the PPR, discrete least-squares best fitting, superconvergence, *a posteriori* error estimator

AMS Subject Classification. 65N30, 65N15, 65N12, 65D10, 74S05, 41A10, 41A25

1 Introduction

Adaptive control based on *a posteriori* error estimates has become standard in finite element methods since the pioneering work by Babuška and Rheinboldt [3]. The field of the *a posteriori* error estimators attracted many researchers and has become the focus of intensive investigations. For the literature, the reader is referred to recent books by Ainsworth and Oden [1] and by Babuška and Strouboulis [4], a conference proceeding [9], a survey article by Bank [5], and an earlier book by Verfürth [12].

Generally speaking, error estimators can be classified under two categories. The residual type estimators (for example, see [6]) constitute the first category while recovery based error estimators (for example, see [17]) constitute the second one. In recovery based estimators, the finite element solution (or its gradient) is postprocessed as a first step. For example, Zienkiewicz and Zhu [18] introduced the Superconvergence Patch Recovery (SPR) that is used to recover a gradient from the gradient of the finite element solution. In another strategy, Wiberg and Li [10, 14] used the finite element solution to build another solution. If the recovered quantity better approximates the exact one, then it can be used in building an asymptotically exact *a posteriori* error estimator (see [1] and [4] for some general discussion and literature).

*This research was partially supported by the National Science Foundation grants DMS-0074301, DMS-0079743, and INT-0196139.

In this work, we consider *a posteriori* error estimators that are based on gradient recovery. As it was shown in [1], if the recovered gradient superconverges to the exact one, the corresponding *a posteriori* error estimator is asymptotically exact. A good example of such estimators is the Zienkiewicz-Zhu error estimator based on the SPR-recovered gradient (see [19]). The Polynomial Preserving Recovery (PPR) is a new gradient recovery technique introduced in [16]. The PPR-recovered gradient, as we shall see soon, has superconvergence properties in mildly structured meshes. Consequently, it can be used in constructing an asymptotically exact *a posteriori* error estimator.

1.1 Model Problem

To fix the ideas, consider the boundary value problem

$$\begin{cases} -\nabla(\mathcal{D}\nabla u + \boldsymbol{b}u) + cu = f & \text{in } \Omega \\ \boldsymbol{n}\cdot(\mathcal{D}\nabla u + \boldsymbol{b}u) = g & \text{on } \Gamma_N \\ u = 0 & \text{on } \Gamma_D \end{cases} \tag{1.1}$$

where $\Omega \subset \mathbb{R}^2$ is a bounded domain with Lipschitz boundary $\partial\Omega = \overline{\Gamma_N} \cup \overline{\Gamma_D}$, the boundary segments Γ_N and Γ_D are disjoint, $\boldsymbol{n}$ is the unit outward normal vector to $\partial\Omega$, and $\mathcal{D}$ is a 2×2 symmetric positive definite matrix. If $\Gamma_N = \partial\Omega, \boldsymbol{b} = 0,$ and $c = 0$, the compatibility condition $\int_\Omega f + \int_{\partial\Omega} g = 0$ must be satisfied and the condition $\int_\Omega u = 0$ is used to ensure the uniqueness. For simplicity, Ω is assumed to be a polygonal domain.

As usual, $W_p^m(\Omega)$ and $H^m(\Omega)$ are the classical Sobolev spaces equipped with the norms $\| \quad \|_{m,p,\Omega}$, and $\| \quad \|_{m,\Omega}$, respectively.

The variational form of this problem is to find $u \in V$ such that

$$\mathcal{B}(u,v) = L(v) \text{ for all } v \in V \tag{1.2}$$

where

$$V = \{v \in H^1(\Omega) : v|_{\Gamma_D} = 0\},$$
$$\mathcal{B}(u,v) = \int_\Omega [(\mathcal{D}\nabla u + \boldsymbol{b}u)\nabla v + cuv]dxdy,$$

and

$$L(v) = \int_\Omega fvdxdy + \int_{\Gamma_N} gvds.$$

If Γ_D is empty, we take $V = H^1(\Omega)$. We assume that the bilinear operator $\mathcal{B}$ is continuous and $V-$elliptic, and the linear operator L is bounded (of course, this requires the problem data to satisfy some conditions). Under these assumptions, the variational problem in (1.2) has a unique weak solution $u \in V$.

Let $\mathcal{T}_h$ be a triangular partition of Ω and let $\mathcal{N}_h$ denote the set of the mesh nodes. The area of a mesh triangle $T \in \mathcal{T}_h$ will be denoted by $|T|$. A mesh node z is called *internal* (*boundary*) mesh node if $z \in \Omega$ ($z \in \partial\Omega$). Consider the C^0 linear finite element space $S_h \subset H^1(\Omega)$ associated with $\mathcal{T}_h$ and defined by

$$S_h = \{v \in H^1(\Omega) : v \in P_1(T) \text{ for every triangle } T \in \mathcal{T}_h\}$$

where $P_r(\mathcal{A})$ denotes the set of all polynomials defined on $\mathcal{A} \subseteq \mathbb{R}^2$ of total degree $\leq r$. The basis functions for S_h are the standard Lagrange basis functions and I_h will denote the Lagrange interpolation operator associated with S_h. The finite element solution of (1.2) is $u_h \in S_h \cap V$ such that

$$\mathcal{B}(u_h, v) = L(v) \text{ for all } v \in S_h \cap V. \tag{1.3}$$

1.2 The SPR and the PPR Techniques

In general, ∇u_h is inherently discontinuous across elements boundaries, and a postprocessing operation is needed to correct this problem. Recovery techniques like the SPR and the PPR can be used for this purpose. The recovered gradient definition in both the SPR and the PPR relies on the following simple observation. The basis functions of S_h are the Lagrange basis functions. Hence, every function in S_h is uniquely defined by its values at the mesh nodes. Let $\{v_z : z \in \mathcal{N}_h\}$ be the Lagrange basis of S_h and let R_h denotes the gradient recovery operator associated with either the SPR or the PPR. Assuming that $R_h u_h$ is defined at every mesh node $z \in \mathcal{N}_h$, the recovered gradient $R_h u_h$ on $\overline{\Omega}$ is defined to be

$$R_h u_h = \sum_{z \in \mathcal{N}_h} R_h u_h(z) v_z.$$

According to this definition, $R_h u_h \in S_h \times S_h$ and it remains to define $R_h u_h$ at the mesh nodes. This is where the SPR and the PPR are different.

Remark 1.1. The definition the SPR and the PPR recovered gradients at mesh nodes involves best fitting operations. In this paper, the best fitting is carried out in discrete least-squares sense.

The definition of the SPR-recovered gradient at $z \in \mathcal{N}_h$ depends on the location of z.

- If $z \in \Omega$, let $\mathcal{K}_z$ denote the patch consisting of the triangles attached to z as shown in Fig. 1(a). Let $p_x \in P_1(\mathcal{K}_z)$ be the linear polynomial that best fits $\partial_x u_h$ at the triangles centroids in $\mathcal{K}_z$. The recovered $x-$derivative at z is defined to be $p_x(z)$. Similarly, we can define the recovered $y-$derivative at z.

- If $z \in \partial\Omega$ is directly connected to no internal mesh nodes, the recovered gradient at z is defined to be $\nabla u_h(z)$.

- If $z \in \partial\Omega$ is directly connected to the internal mesh nodes $z_1, z_2, \ldots, z_{N_z}$, let $\mathcal{K}_{z_i}$ be the patch associated with z_i. Again, $\mathcal{K}_{z_i}$ consists of the mesh triangles that are directly attached to z_i. Let $p_{x,z_i} \in P_1(\mathcal{K}_{z_i})$ be the linear polynomial that best fits $\partial_x u_h$ at the triangles centroids in $\mathcal{K}_{z_i}$. The recovered $x-$derivative at z is defined to be $\dfrac{1}{N_z}\displaystyle\sum_{i=1}^{N_z} p_{x,z_i}(z)$. Similarly, we can define the recovered $y-$derivative at z.

Next, we turn our attention to the definition of the PPR-recovered gradient at $z \in \mathcal{N}_h$. Starting with a patch $\mathcal{K}_z$, let $p \in P_2(\mathcal{K}_z)$ be the quadratic polynomial that best fits u_h at the mesh nodes in $\mathcal{K}_z$. The PPR-recovered gradient at z is defined to be $\nabla p(z)$. The construction of $\mathcal{K}_z$ is not straight forward as in the SPR. As we will see soon, $\mathcal{K}_z$ must have at least 6 mesh nodes that are not on a conic section. This is to guarantee the existence and the uniqueness of of p. Indeed, the construction of $\mathcal{K}_z$ starts by the patch $\mathcal{K}_{z,0}$ that consists of the mesh triangles directly attached with z. The next construction step depends on the location of z.

- If $z \in \Omega$ and $\mathcal{K}_{z,0}$ has at least 5 mesh triangles, then $\mathcal{K}_z = \mathcal{K}_{z,0}$ as shown in Fig. 1(a).

- If $z \in \Omega$ and $\mathcal{K}_{z,0}$ has 3 or 4 mesh triangles, then

$$\mathcal{K}_z = \mathcal{K}_{z,0} \cup \{T \in \mathcal{T}_h : T \cap \mathcal{K}_{z,0} \text{ is an edge of } T\}$$

  as shown in Fig. 1(b).

- If $z \in \partial\Omega$ and $\mathcal{K}_{z,0}$ has at least one internal mesh node

$$\mathcal{K}_z = \mathcal{K}_{z,0} \cup \{\mathcal{K}_{\hat{z}} : \hat{z} \in \mathcal{K}_{z,0} \text{ is an internal mesh node}\} \tag{1.4}$$

  as shown in Fig. 2(a). If $\mathcal{K}_{z,0}$ has no internal mesh nodes, replace $\mathcal{K}_{z,0}$ in (1.4) by a bigger patch

$$\mathcal{K}_{z,1} = \bigcup\{\mathcal{K}_{\hat{z},0} : \hat{z} \in \mathcal{K}_{z,0} \text{ is a mesh node }\}. \tag{1.5}$$

  An example of this situation is depicted in Fig. 2(b). Practically, $\mathcal{K}_{z,1}$ must have at least one internal mesh node. If this is not the case, iterate the extension process in (1.5).

Having introduced the definitions of the SPR and the PPR, we have the following remarks.

1. The main difference between the SPR and the PPR is that the SPR works on ∇u_h while the PPR works on u_h.

2. The PPR has good approximation properties as it satisfies the *consistency condition*. A recovery operator R_h is said to satisfy the consistency condition if

$$R_h(I_h p) = \nabla p \quad \forall p \in P_2(\Omega). \tag{1.6}$$

   If R_h satisfies (1.6), Bramble-Hilbert Lemma can be used to show that

$$\|\nabla u - R_h I_h u\|_{L^\infty(\Omega)} \leq Ch^2 |u|_{3,\infty,\Omega} \quad \forall u \in W^3_\infty(\Omega)$$

   where $C > 0$ is some constant independent of u and h (see [16] for more details). The PPR satisfies (1.6) because the the best fit polynomials over individual patches and the original polynomial are typically the same. On the other hand, the SPR does not satisfy the consistency condition unless $\mathcal{T}_h$ has some special structure.

3. Basically, the PPR can be viewed as a dynamic way to generate difference formulas for first order partial derivatives. The generated formulas can recover the exact derivatives of quadratic polynomials. Babuška and Strouboulis [4] proposed a technique to generate such kind of difference formulas *a priori* (see Example 4.8*.4 in [4]), but this technique is not suitable for real time computations on real meshes.

4. The idea of best fitting the nodal values of u_h by a quadratic polynomial is well known in engineering applications. For example, Wiberg and Li [10, 14] used this idea in constructing a recovered solution $\tilde{u}_h$ from u_h. According to their strategy, the true error $\|u - u_h\|_{L^2(T)}$ on $T \in \mathcal{T}_h$ is estimated using $\|\tilde{u}_h - u_h\|_{L^2(T)}$. Indeed, Wiberg and Li were mainly concerned about estimating the error and not recovering the gradient.

5. The PPR gradient recovery can be easily extended to higher order elements and to problems in $\mathbb{R}^3$. This will be the topic of a future work that would be available soon.

1.3 Gradient Recovery and The Superconvergence Property

As it was mentioned before, if the recovered gradient enjoys the superconvergence property, then it can be used in building an asymptotically exact *a posteriori* error estimator. Ainsworth and Oden [1] established a general framework that can be used in proving the superconvergence property, if it exists. Let R_h denote the recovery operator associated with a gradient recovery technique. According to this framework, there are three main requirements to show that $R_h u_h$ superconverges to ∇u.

1. R_h satisfies the consistency condition.

2. The recovery operator R_h is bounded in the following sense:

$$\|R_h v\|_{L^2(T)} \leq C|v|_{1,\mathcal{K}_T} \qquad \forall T \in \mathcal{T}_h \text{ and } \forall v \in S_h \tag{1.7}$$

   where $\mathcal{K}_T$ is a patch of triangles containing T.

3. ∇u_h enjoys superconvergence in the following sense:

$$\|\nabla(I_h u - u_h)\|_{L^2(\Omega)} \leq Ch^{1+\rho} \tag{1.8}$$

   for some $\rho \in (0,1]$ and some constant $C > 0$ that is independent of h.

If u_h and R_h satisfies the above requirements, then it is possible to prove that

$$\|\nabla u - R_h u_h\|_{L^2(\Omega)} \leq Ch^{1+\rho}. \tag{1.9}$$

With this result in hand, it is straight forward to prove that the *a posteriori* error estimator

$$\eta_h = \|R_h u_h - \nabla u_h\|_{L^2(\Omega)} \tag{1.10}$$

is asymptotically exact.

From this point on, we will concentrate on the PPR and its corresponding operator which we will denote by $\mathrm{G^h}$. Our target in this paper is to show that $\mathrm{G^h} u_h$ superconverges to ∇u following the above framework. By construction, and as it was explained before, $\mathrm{G^h}$ satisfies the first requirement. For the third requirement, Xu and Zhang [15] had recently established (1.8) for a wide range of meshes that are mildly structured in the sense of the following definition.

Definition 1.2. *The triangulation $\mathcal{T}_h$ is said to satisfy the* <u>condition (α,σ)</u> *if there exists a partition $\mathcal{T}_{h,1} \cup \mathcal{T}_{h,2}$ of $\mathcal{T}_h$ and positive constants α and σ such that every two adjacent triangles in $\mathcal{T}_{h,1}$ form an $O(h^{1+\alpha})$ parallelogram and $\sum_{T\in\mathcal{T}_{h,2}} |T| = O(h^\sigma)$.*

An $O(h^{\alpha+1})$ parallelogram is a quadrilateral in which the difference between the lengths of any two opposite sides is $O(h^{\alpha+1})$. When $\alpha = \infty$, every pair of adjacent triangles in $\mathcal{T}_{h,1}$ form a parallelogram. When $\alpha = \sigma = \infty$, $\mathcal{T}_h$ is uniformly generated by lines parallel to three fixed directions. This case was handled in [11, 8] where $u - u_h$ was expanded at mesh nodes, and the case in which $\alpha = 1$ was handled in [7]. For general α and σ, Xu and Zhang [15] proved the following theorem.

Theorem 1.3. *Let u be the solution of* (1.2)*, let $u_h \in S_h$ be the finite element solution of* (1.3)*, and let $I_h u \in S_h$ be the linear interpolation of u. If the triangulation $\mathcal{T}_h$ satisfies the condition (α, σ) and $u \in H^3(\Omega) \cap W^2_\infty(\Omega)$, then*

$$\|u_h - I_h u\|_{1,\Omega} \leq h^{1+\rho}(\|u\|_{3,\Omega} + |u|_{2,\infty,\Omega}),$$

where $\rho = \min(\alpha, \frac{1}{2}, \frac{\sigma}{2})$.

Remark 1.4. The condition(α, σ) is sufficient to guarantee the superconvergence result in (1.8), although it is not necessary as we shall see in the numerical examples. Nevertheless, this condition is satisfied for meshes generated by many automatic mesh generators as described in [15].

The second requirement is somewhat easy to establish when the recovery technique works directly on the gradient as in weighted average recovery and the SPR. However, the situation is much harder for the PPR as it works on function values. It is not even clear how to relate $\mathrm{G^h} v$ to ∇v, where $v \in S_h$. Actually, the core of this paper is devoted for showing that $\mathrm{G^h}$ satisfies the third requirement. Having this result paves the way to show that $\mathrm{G^h}$ enjoys the superconvergence property in (1.9) and that the error estimator η_h is asymptotically exact. At the end of the paper, some numerical examples are provided to practically show that the PPR-recovered gradient superconverges to the exact gradient.

2 Definition and existence of $\mathrm{G^h}$

As mentioned before, the construction of $\mathrm{G^h} v \in S_h \times S_h$ for a function $v \in S_h$ is complete if $(\mathrm{G^h} v)(z)$ is defined for every $z \in \mathcal{N}_h$. Therefore, it suffices to address the definition and existence questions at the level of mesh nodes.

Consider a mesh node z and let $\mathcal{K}_z$ denote its corresponding patch. In the patch $\mathcal{K}_z$, let $T_1, T_2, \ldots, T_m$ denote the mesh triangles and let $z_0 = (x_0, y_0), z_1 = (x_1, y_1), \ldots, z_n = (x_n, y_n)$ denote the mesh nodes. Without loss of generality, let $z = z_0$. Let $h_z = \max\{\|z_i - z_0\| : 1 \leq i \leq n\}$. To avoid the computational instability associated with small h_z, the computations will be carried out on the patch

$$\omega_z = F_z(\mathcal{K}_z) \text{ where } F_z : (x, y) \rightarrow (\hat{x}, \hat{y}) = \frac{(x, y) - (x_0, y_0)}{h_z}. \tag{2.1}$$

The patch ω_z will be called *the reference patch associated with* z. For $0 \leq i \leq n$, let $\hat{z}_i = (\hat{x}_i, \hat{y}_i) = F(z_i)$ and set $v_i = (v \circ F_z^{-1})(\hat{z}_i) = v(z_i)$. Let $p_z \in P_2(\omega_z)$ be the quadratic polynomial that best fits the data points $\{(\hat{z}_i, v_i) : 0 \le i \le n\}$. For $(\hat{x}, \hat{y}) \in \omega_z$, $p_z(\hat{x}, \hat{y})$ can be written in the form

$$p_z(\hat{x}, \hat{y}) = \hat{\boldsymbol{x}}^T \boldsymbol{c_z}$$

where $\boldsymbol{c}_z$ is the coefficients vector $\begin{bmatrix} c_{z,1} & c_{z,2} & c_{z,3} & c_{z,4} & c_{z,5} & c_{z,6} \end{bmatrix}^T$ and $\hat{\boldsymbol{x}}$ is the monomials vector $\begin{bmatrix} 1 & \hat{x} & \hat{y} & \hat{x}^2 & \hat{x}\hat{y} & \hat{y}^2 \end{bmatrix}^T$. Since we are using discrete least-squares fitting, the coefficients vector $\boldsymbol{c}_z$ is determined by the linear system

$$A_z^T A_z \boldsymbol{c}_z = A_z^T \boldsymbol{v}_z$$

where

$$A_z = \begin{bmatrix} \hat{\boldsymbol{x}}_0^T \\ \hat{\boldsymbol{x}}_1^T \\ \hat{\boldsymbol{x}}_2^T \\ \vdots \\ \hat{\boldsymbol{x}}_n^T \end{bmatrix}, \hat{\boldsymbol{x}}_i = \begin{bmatrix} 1 \\ \hat{x}_i \\ \hat{y}_i \\ \hat{x}_i^2 \\ \hat{x}_i\hat{y}_i \\ \hat{y}_i^2 \end{bmatrix} \text{ for } 0 \le i \le n, \text{ and } \boldsymbol{v}_z = \begin{bmatrix} v_0 \\ v_1 \\ v_2 \\ \vdots \\ v_n \end{bmatrix}. \tag{2.2}$$

Set

$$B_z = A_z^T A_z,$$

then, assuming the existence of B_z^{-1},

$$\boldsymbol{c}_z = B_z^{-1} A_z^T \boldsymbol{v}_z.$$

By definition,

$$\mathrm{G^h} v(z) = \frac{1}{h_z} \begin{bmatrix} \partial_{\hat{x}} p_z(0,0) & \partial_{\hat{y}} p_z(0,0) \end{bmatrix}^T.$$

Therefore,

$$\mathrm{G^h} v(z) = \frac{1}{h_z} \begin{bmatrix} c_{z,2} & c_{z,3} \end{bmatrix}^T = \frac{1}{h_z} \begin{bmatrix} \boldsymbol{v}_z^T A_z B_z^{-1} e_2 & \boldsymbol{v}_z^T A_z B_z^{-1} e_3 \end{bmatrix}^T \tag{2.3}$$

where e_2 and e_3 are the second and the third columns of the identity matrix $I_{6\times 6}$.

To this end, it is important to address the following question: are there any sufficient conditions that guarantee the existence of B_z^{-1}? The answer of this question relies on the following simple proposition.

Proposition 2.1.

1. *If B_z is not invertible, then there is a conic section passing through the mesh nodes in $\mathcal{K}_z$.*
2. *Any tangent to a branch of a hyperbola can not intersect with the other branch.*

Proof. If B_z is not invertible, then $\boldsymbol{c}_z$ has infinitely many solutions. Therefore, there are infinitely many polynomials in $P_2(\omega_z)$ that pass through the data points $\{(\hat{z}_i, v_i) : 0 \leq i \leq n\}$. Let $p_{z,1}$ and $p_{z,2}$ be two of such polynomials and let $q = p_{z,1} - p_{z,2}$. Then, $q(\hat{z}_i) = 0$ for $0 \leq i \leq n$ and the conic section $\{(\hat{x}, \hat{y}) : q_z(\hat{x}, \hat{y}) = 0\}$ passes through $\{\hat{z}_i : 0 \leq i \leq n\}$. Since conic sections are invariant under affine mappings, the proof of the first part is complete. The proof of the second part is elementary. □

Definition 2.2. *The patch $\mathcal{K}_z$ (or ω_z) is said to satisfy the angle condition if the sum of any two adjacent angles inside $\mathcal{K}_z$ is at most π, and is said to satisfy the line condition if its mesh nodes are not lying on two lines.*

Let n_1 denotes the number of mesh nodes that are directly connected to z and set $n_2 = n - n_1$. If $z \in \Omega$, then $n_1 \geq 3$. Practically, a good mesh generator can detect any node z for which $n_1 = 3$ and removes it. So, we may assume that $n_1 \geq 4$. It is obvious that for an internal mesh node z with $n_1 > 4$, $\mathcal{K}_z$ automatically satisfies the line condition. If $n_1 = 4$, $\mathcal{K}_z$ may violate this condition as shown in Fig. 4.

The following theorem plays the crucial part in proving the boundedness of $\mathrm{G^h}$.

Theorem 2.3. *Let z be an internal mesh node with $n_1 \geq 4$ and let $\mathcal{K}_z$ be its corresponding patch that satisfies the angle condition. Additionally, let $\mathcal{K}_z$ satisfy the line condition when $n_1 = 4$. Then, B_z is invertible.*

Proof. By the first part of Proposition 2.1, it suffices to show that $\mathcal{K}_z$ has six distinct nodes that are not on a conic section. Since $z \in \Omega$, the sum of the angles at z is 2π. Hence, the nodes in $\mathcal{K}_z$ can not lie on a circle, on a parabola, on an ellipse, or on one branch of a hyperbola. Since $\mathcal{K}_z$ satisfies the line condition, the nodes can not be on two lines. The remaining possibility is to have the nodes distributed on two branches of a hyperbola. Depending on n_1, we can have one of the following two cases.

Case 1: $n_1 = 4$. In this case the triangles attached to z_0 form a quadrilateral as shown in Fig. 4. Since $\mathcal{K}_z$ satisfies the angle condition, z_0 must be the intersection point of the quadrilateral diagonals. Hence, the nodes in $\mathcal{K}_z$ can not be distributed on two branches of a hyperbola as a line intersects with a hyperbola at no more than two points.

Case 2: $n_1 > 4$. Proceed by contradiction and assume that the nodes in $\mathcal{K}_z$ are distributed on two branches of a hyperbola. Without loss of generality, assume that the real axis of the hyperbola is horizontal and that z_0 is on the right branch of the hyperbola. The left branch can not have more than two mesh nodes. If it has three nodes as in Fig. 3(a), then the sum of the angles at z_2 is more than π.

If the left branch has two nodes, then $\mathcal{K}_z$ must have nodes z_3 and z_4 on the right branch as shown in Fig. 3(b). We claim that $\mathcal{K}_z$ can not have any more nodes on the right branch. If this claim is true, $\mathcal{K}_z$ will have $n_1 = 4$ and this is a contradiction as $n_1 > 4$ by assumption. To prove the previous claim, assume that $\mathcal{K}_z$ has another node z_5 as in Fig. 3(b). Then, the sum of the angles at node z_3 is greater than π unless the nodes z_1, z_3, and z_5 lie on a line that is tangent to the right branch of the hyperbola, which is impossible by the second part of Proposition 2.1.

The only remaining possibility is to have exactly one node on the left branch of the hyperbola as in Fig. 3(c). Again, by an argument similar to the one used in previous case, this leads to a contradiction. $\square$

Corollary 2.4. *Consider a boundary mesh node z and let $\mathcal{K}_z$ be its corresponding patch. Suppose that $\mathcal{K}_z$ contains another patch $\mathcal{K}_{\hat{z}}$ corresponding to an internal mesh node $\hat{z}$. If $\mathcal{K}_{\hat{z}}$ satisfies the angle and the line conditions, then B_z is invertible.*

3 Boundedness of G^{h}

Let $v \in S_h$, let $\mathcal{K}_z$ be the patch associated with $z \in \mathcal{N}_h$, and consider the mesh triangle $T_k \subset \mathcal{K}_z$ for some $1 \le k \le m$. Let the vertices of T_k be $(x_{k,1}, y_{k,1})$, $(x_{k,2}, y_{k,2})$, and $(x_{k,3}, y_{k,3})$, where the numbering is in counterclockwise direction. Since $v \in P_1(T_k)$, it is easy to verify that

$$\partial_x v(x,y) = \sum_{j=1}^{3} a_{k,j} v_{k,j} \text{ and } \partial_y v(x,y) = \sum_{j=1}^{3} b_{k,j} v_{k,j} \text{ for } (x,y) \in T_k \tag{3.1}$$

where

$$a_{k,j} = \frac{1}{2|T_k|}(y_{k,j+1} - y_{k,j+2}), b_{k,j} = \frac{1}{2|T_k|}(x_{k,j+2} - x_{k,j+1}), v_{k,j} = v(x_{k,j}, y_{k,j}),$$

and the addition in indices is mod 3. Equivalently,

$$\partial_x v(x,y) = \boldsymbol{v}_k^T \boldsymbol{a}_k \text{ and } \partial_y v(x,y) = \boldsymbol{v}_k^T \boldsymbol{b}_k \text{ for } (x,y) \in T_k$$

where $\boldsymbol{a}_k = \begin{bmatrix} a_{k,1} & a_{k,2} & a_{k,3} \end{bmatrix}^T$, $\boldsymbol{b}_k = \begin{bmatrix} b_{k,1} & b_{k,2} & b_{k,3} \end{bmatrix}^T$, and $\boldsymbol{v}_k = \begin{bmatrix} v_{k,1} & v_{k,2} & v_{k,3} \end{bmatrix}^T$. Let E_k be an $(n+1) \times 3$ Boolean matrix defined for T_k, where

$$E_k(i,j) = \begin{cases} 1 & \text{if the node } i \text{ in } \mathcal{K}_z \text{ is the vertex } j \text{ in } T_k \\ 0 & \text{otherwise} \end{cases}.$$

Then,

$$\boldsymbol{v}_k = E_k^T \boldsymbol{v}_z$$

and (3.1) can be simplified to the form

$$\partial_x v(x,y) = \boldsymbol{v}_z^T E_k \boldsymbol{a}_k \text{ and } \partial_y v(x,y) = \boldsymbol{v}_z^T E_k \boldsymbol{b}_k \text{ for } (x,y) \in T_k. \tag{3.2}$$

Let ω_z be the reference patch associated with z and let F_z be the affine mapping from $\mathcal{K}_z$ to ω_z. Let $\hat{T}_k = F_z(T_k)$ and let $(\hat{x}_{k,j}, \hat{y}_{k,j}) = F_z(x_{k,j}, y_{k,j})$ for $1 \le j \le 3$. It is easy to verify that

$$a_{k,j} = \frac{\hat{a}_{k,j}}{h_z} \text{ and } b_{k,j} = \frac{\hat{b}_{k,j}}{h_z}$$

where

$$\hat{a}_{k,j} = \frac{1}{2|\hat{T}_k|}(\hat{y}_{k,j+1} - \hat{y}_{k,j+2}) \text{ and } \hat{b}_{k,j} = \frac{1}{2|\hat{T}_k|}(\hat{x}_{k,j+2} - \hat{x}_{k,j+1}).$$

Let $\hat{\boldsymbol{a}}_k = \begin{bmatrix} \hat{a}_{k,1} & \hat{a}_{k,2} & \hat{a}_{k,3} \end{bmatrix}^T$ and $\hat{\boldsymbol{b}}_k = \begin{bmatrix} \hat{b}_{k,1} & \hat{b}_{k,2} & \hat{b}_{k,3} \end{bmatrix}^T$, then (3.2) can be rewritten in the form

$$\partial_x v(x,y) = \frac{\boldsymbol{v}_z^T E_k \hat{\boldsymbol{a}}_k}{h_z} \text{ and } \partial_y v(x,y) = \frac{\boldsymbol{v}_z^T E_k \hat{\boldsymbol{b}}_k}{h_z} \text{ for } (x,y) \in T_k. \tag{3.3}$$

Let $\mathrm{G^h}_1\, v$ and $\mathrm{G^h}_2\, v$ stand for the recovered $x-$ and $y-$derivatives, respectively. Establishing the boundedness of $\mathrm{G^h}$ in the sense of (1.7) would be easy if $\mathrm{G^h}_l\, v(z)$ can be expressed as a linear combination of the first partial derivatives of v on the triangles of ω_z for $l = 1, 2$. So, we will try to find a set of *bounded values* $\alpha_{z,l,1}, \ldots, \alpha_{z,l,m}, \beta_{z,l,1}, \ldots, \beta_{z,l,m}$ such that

$$\mathrm{G^h}_l\, v(z) = \sum_{k=1}^{m} [\alpha_{z,l,k}(\partial_x v)_k + \beta_{z,l,k}(\partial_y v)_k] \text{ for } l = 1, 2 \tag{3.4}$$

where $(\partial_x v)_k$ and $(\partial_y v)_k$ are the first partial derivatives of v in T_k. Using Equations (2.3) and (3.3) in Equation (3.4), we get

$$\boldsymbol{v}_z^T \sum_{k=1}^{m} [\alpha_{z,l,k} E_k \hat{\boldsymbol{a}}_k + \beta_{z,l,k} E_k \hat{\boldsymbol{b}}_k] = \boldsymbol{v}_z^T A_z B_z^{-1} e_{l+1} \text{ for } l = 1, 2.$$

Setting

$$M_z = \begin{bmatrix} E_1 \hat{\boldsymbol{a}}_1 & \cdots & E_m \hat{\boldsymbol{a}}_m & E_1 \hat{\boldsymbol{b}}_1 & \cdots & E_m \hat{\boldsymbol{b}}_m \end{bmatrix} \tag{3.5}$$

and

$$\boldsymbol{\gamma}_{z,l} = \begin{bmatrix} \alpha_{z,l,1} & \cdots & \alpha_{z,l,m} & \beta_{z,l,1} & \cdots & \beta_{z,l,m} \end{bmatrix}^T,$$

we get

$$\boldsymbol{v}_z^T M_z \boldsymbol{\gamma}_{z,l} = \boldsymbol{v}_z^T A_z B_z^{-1} e_{l+1} \text{ for } l = 1, 2.$$

Since this is true for all $v \in S_h$,

$$M_z \boldsymbol{\gamma}_{z,l} = A_z B_z^{-1} e_{l+1} \text{ for } l = 1, 2. \tag{3.6}$$

Note that the order of M_z is $(n+1) \times (2m)$.

Lemma 3.1. *Consider $z \in \mathcal{N}_h$. If the patch $\mathcal{K}_z$ corresponding to z has no degenerate triangles and B_z is invertible, then* $\operatorname{Rank} M_z = n$ *and the system in* (3.6) *has infinitely many solutions.*

Proof. Since $\mathcal{K}_z$ is simply connected, then, using Euler's theorem, $(n+1) - e + m = 1$, where e is the number of edges in $\mathcal{K}_z$. Hence, $(n+1) - 2m = e - 3m + 1$. By a simple induction argument on m, we can show that $e - 3m + 1 < 0$ for $m \geq 3$. Hence, the system in (3.6) is underdetermined.

To prove that $\operatorname{Rank} M_z = n$, consider the homogeneous linear system

$$M_z^T \boldsymbol{w} = 0, \tag{3.7}$$

with $\boldsymbol{w} = \begin{bmatrix} w_0 & w_1 & \cdots & w_n \end{bmatrix}^T$. We can view $w_0, w_1, \ldots, w_n$ as the nodal values of some function $w \in S_h$ at the nodes $z_0, z_1, \ldots, z_n$ in $\mathcal{K}_z$. With this in mind, the homogeneous system in (3.7) implies that $\nabla w = 0$ in T_k for $k = 1, 2, \ldots, m$. Hence, w is constant on $\mathcal{K}_z$, as $w \in S_h$, and $w_0 = w_1 = \cdots = w_n$ in any solution $\boldsymbol{w}$ of (3.7). Consequently, the dimension of the null space of M_z^T is 1 and $\operatorname{Rank} M_z^T = \operatorname{Rank} M_z = n$. Moreover, the only row operation on M_z that leads to a row of zeros is adding all the rows together. Since $\mathrm{G^h}$ recovers the exact gradient for any polynomial $p \in P_2(\omega_z)$, it is easy to verify that the row sum of $A_z B_z^{-1} e_{l+1}$ is 0 for $l = 1, 2$. Therefore, the homogeneous system in (3.6) is consistent for $l = 1, 2$. □

Among all the solutions of (3.6), we consider the one with the minimum length given by

$$\boldsymbol{\gamma}_{z,l}^* = M_z^\dagger A_z B_z^{-1} e_{l+1} \text{ for } l = 1, 2 \tag{3.8}$$

where $M_z^\dagger$ is the pseudoinverse of M_z. For every mesh triangle T, define the patch

$$\mathcal{K}_T = \bigcup \{\mathcal{K}_z : z \text{ is a vertex of } T\}.$$

For any Matrix $K \in \mathbb{R}^{k_1 \times k_2}$, let $\sigma_1(K)$ and $\sigma_{\min(k1,k2)}(K)$ denote the largest and the smallest singular values of K, respectively. Recall that $\sigma_l^2(K) = \sigma_l(K^T K)$ for $l = 1, 2, \ldots, \min(k1, k2)$.

Theorem 3.2. *Let $0 < C_1 \leq \sigma_6(A_z) \leq \sigma_1(A_z) \leq C_2$ and $0 < C_3 \leq \sigma_n(M_z)$ for every mesh node $z \in \mathcal{N}_h$ and for some constants C_1, C_2, and C_3 that are independent of h. Then, there exists a constant C, independent of h, such that*

$$\| \mathrm{G^h} v \|_{L^2(T)} \leq C |v|_{1,\mathcal{K}_T} \tag{3.9}$$

for all $T \in \mathcal{T}_h$ and for all $v \in S_h$.

Proof. Consider a mesh triangle T and let $\mathcal{K}_T$ be the patch corresponding to T. Let z be a vertex of T and consider any $v \in S_h$. Using equations (3.4) and (3.8) we get

$$\begin{aligned} |\, \mathrm{G^h}_l\, v(z)| &\leq \|\boldsymbol{\gamma}_l^*\|_1 |v|_{1,\infty,\mathcal{K}_z} \leq c_1 \|\boldsymbol{\gamma}_l^*\|_2 |v|_{1,\infty,\mathcal{K}_T} \\ &\leq c_2 \|M^\dagger\|_2 \|A\|_2 \|B^{-1}\|_2 |v|_{1,\infty,\mathcal{K}_T} \\ &\leq \frac{c_2 C_2}{C_3 C_1^2} |v|_{1,\infty,\mathcal{K}_T} \end{aligned}$$

for $l = 1, 2$. Since $\mathrm{G^h} v \in P_1(T) \times P_1(T)$,

$$\| \mathrm{G^h} v\|_{L^\infty(T)} \leq C|v|_{1,\infty,\mathcal{K}_T}.$$

Hence,

$$\begin{aligned} \| \mathrm{G^h} v\|_{L^2(T)} &\leq \sqrt{|T|}\| \mathrm{G^h} v\|_{L^\infty(T)} \leq C\, \mathrm{diam}(T)|v|_{1,\infty,\mathcal{K}_T} \\ &\leq C\frac{\mathrm{diam}(T)}{\mathrm{diam}(\mathcal{K}_T)}|v|_{1,\mathcal{K}_T} \leq C|v|_{1,\mathcal{K}_T}. \end{aligned} \tag{3.10}$$

The inequality in (3.10) is obtained using an inverse estimate. □

It is obvious that the bounds assumed about the singular values of A_z and M_z in Theorem 3.2 depend on the mesh geometry as shown in the following theorem.

Theorem 3.3. *Let $\mathcal{T}_h$ be a triangular partition of Ω that satisfies the following conditions.*

1. *There exists a finite positive integer N such that $n_1 \leq N \, \forall z \in \mathcal{N}_h$, and $n_1 \geq 4$ if $z \in \Omega$.*

2. *The sum of any two adjacent angles at $z \in \mathcal{N}_h$ is π if $z \in \Omega$ with $n_1 = 4$, and is at most π if $z \in \partial\Omega$ or if $z \in \Omega$ with $n_1 > 4$.*

3. *If $z \in \Omega$ with $n_1 = 4$, then the sum of the two adjacent angles in $\mathcal{K}_z$ at one of the mesh nodes directly connected to z is at most $\pi - \phi$ for some $0 < \phi < \pi$.*

4. *If $\theta_{min,h}$ and $\theta_{max,h}$ are the smallest and the largest angles in $\mathcal{T}_h$, respectively, then there exist constants $\underline{\phi}$ and $\overline{\phi} < \pi$ such that*

$$0 < \underline{\phi} \leq \theta_{min,h} \leq \theta_{max,h} \leq \overline{\phi} < \pi.$$

5. *Every boundary mesh node z is connected to an internal mesh node $\bar{z}$ either directly or indirectly through at most one boundary mesh node.*

Then, there exist constants C_1, C_2, and C_3, independent of h, such that

$$0 < C_1 \leq \sigma_6(A_z) \leq \sigma_1(A_z) \leq C_2 \text{ and } 0 < C_3 \leq \sigma_n(M_z) \quad \forall z \in \mathcal{N}_h.$$

Remark 3.4. The third condition in Theorem 3.3 is imposed to avoid the singular situation shown in Fig. 4. Also, the fifth condition can be relaxed.

Proof. Let $z \in \mathcal{N}_h$ and let D denote the closed unit disk centered at (0,0). Since the reference patch $\omega_z \subset D$, $|B_z(i,j)| \leq (n+1)$ for $1 \leq i, j \leq 6$. Hence,

$$\sigma_1(A_z) = \sqrt{\sigma_1(B_z)} \leq \sqrt{\sigma_1(|B_z|)} \leq \sqrt{6(n+1)}.$$

By the first and the fifth conditions, it is easy to verify that $n \leq N$ if $z \in \Omega$, $n \leq N^2 - 5N + 10$ if $z \in \partial\Omega$ and z is directly attached to an internal node, and $n \leq 3N - 2$ if $z \in \partial\Omega$ and z is indirectly attached to an internal node through a third boundary node. Hence, there exists $C_2 = C_2(N)$ such that $\sigma_1(A_z) \leq C_2$.

To establish the existence of C_1, let us first consider the internal nodes. Let ω_z be a reference patch associated with an internal mesh node z. By definition, $\omega_z \subset D$, ω_z has a node at $(0,0)$, and ω_z has at least one node on ∂D. The first four conditions imply that ω_z has no degenerate triangles and that ω_z satisfies the line and the angle conditions. To show that $\inf\{\sigma_6(A_z) : z \in \mathcal{N}_h \cap \Omega\} \geq C_1 > 0$ for any $h > 0$, proceed by contradiction and assume that there exits a sequence of reference patches $\{\omega_i\}_{i=1}^{\infty}$ such that ω_i has all the properties of ω_z for all $i \geq 1$ and $\sigma_6(A_i) \to 0$, where A_i is the matrix defined for ω_i as in (2.2). Without loss of generality, and by the first condition, one may assume n and n_1 are the same for any patch ω_i; otherwise we may pass to a subsequence. For $i \geq 1$, the nodes in ω_i are $\tilde{z}_{i,0} = (0,0), \tilde{z}_{i,1}, \tilde{z}_{i,2}, \ldots, \tilde{z}_{i,n}$. According to n_1, we have two cases.

Case 1: $n_1 > 4$. By compactness of D, one may assume that $\tilde{z}_{i,j} \to \tilde{z}_j \in D$ for $0 \leq j \leq n$; otherwise one may pass to a subsequence. The nodes $\tilde{z}_0 = (0,0), \tilde{z}_1, \tilde{z}_2, \ldots, \tilde{z}_n$ can be viewed as the nodes of a patch ω whose pattern is similar to the one shown in Fig. 5(a). Using the properties of ω_i, non of the triangles in ω is degenerate, ω has at least one node on ∂D, and the sum of any two adjacent angles in ω can not exceed π. Hence, ω satisfies the angle and the line conditions. If A denotes the matrix defined for ω as in (2.2), then $\sigma_6(A) \neq 0$. Since $\tilde{z}_{i,j} \to \tilde{z}_j$ for all $0 \leq j \leq n$, $A_i \to A$ in any matrix norm. Hence, $0 \neq \sigma_6(A) = \lim_{i\to\infty} \sigma_6(A_i) = 0$, which is a contradiction.

Case 2: $n_1 = 4$. Since ω_i satisfies the angle condition, it contains 4 nodes that are corners of a convex quadrilateral whose diagonals intersect at $\tilde{z}_{i,0} = (0,0)$. Denote the the quadrilateral in ω_i by Q_i and denote the set of its diagonals by ℓ_i. Since one of the nodes in ω_i is on ∂D, it is easy to verify that Q_i inscribes a circle whose radius is at least $\delta = \delta(\underline{\phi})$ for some $\delta > 0$ and for all $i \geq 1$. Consequently,

$$\max\{\mathrm{dist}(\tilde{z}_{i,j}, \ell_i) : 0 \leq j \leq n\} \geq \delta \sin(\phi) > 0 \tag{3.11}$$

Since D is Compact, assume that $\tilde{z}_{i,j} \to \tilde{z}_j$ for $0 \leq j \leq n$. The nodes $\tilde{z}_0 = (0,0), \tilde{z}_1, \tilde{z}_2, \ldots, \tilde{z}_n$ can be viewed as the nodes of a patch ω similar to one of the patterns shown in Fig. 5(b-e). The patch ω has a quadrilateral denoted by Q and the diagonals of Q are denoted by ℓ. The corners Q are the limits of the corners in Q_i. Hence, (3.11) leads to

$$\max\{\mathrm{dist}(\tilde{z}_j, \ell) : 0 \leq j \leq n\} \geq \delta \sin(\phi),$$

and ω satisfies the line and the angle conditions. As in previous case, this leads to a contradiction.

Let us turn our attention to the boundary mesh nodes, and let $\mathcal{K}_z$ be the patch corresponding to a boundary mesh node z. By construction, $\mathcal{K}_z$ contains, at least, one patch $\mathcal{K}_{\bar{z}}$ corresponding to an internal mesh node $\bar{z}$. By the fifth condition, $\bar{z}$ is either connected to z directly or indirectly through a third boundary mesh node $\tilde{z}$. As before, $\mathcal{K}_z$ is a subset of a disk centered at z and its radius is h_z. Hence, and without loss of generality, there exists a mesh node $z^* \in \mathcal{K}_{\bar{z}}$, as shown in Fig. 2, such that

$$\|z - \bar{z}\| + \|\bar{z} - z^*\| \geq \|z - z^*\| = h_z.$$

This implies that $\max(\|z - \bar{z}\|, \|\bar{z} - z^*\|) \geq h_z/2$. If z is directly connected to $\bar{z}$ as in Fig. 2(a), then $\mathrm{diam}(\mathcal{K}_{\bar{z}}) \geq h_z$. If z is indirectly connected to $\bar{z}$ as in Fig. 2(a), then we have two situations depending on whether $\|\bar{z} - z^*\| \geq h_z/2$ or $\|z - \bar{z}\| \geq h_z/2$. In the former situation $\mathrm{diam}(\mathcal{K}_{\bar{z}}) \geq h_z$, and for the later situation consider the triangle $z\tilde{z}\bar{z}$. In this triangle the angle at z is at least $\underline{\phi}/2$ by the fourth condition, and hence $\|\bar{z} - \tilde{z}\| \geq h_z \sin(\underline{\phi}/2)/2$. If not, we can use the triangle $z\acute{z}\bar{z}$. Consequently, $\mathrm{diam}(\mathcal{K}_{\bar{z}}) \geq h_z \sin(\underline{\phi}/2)$.

Hence, the reference patch ω_z contains a patch $\bar{\omega}$ that is a scaled translation of the reference patch $\omega_{\bar{z}}$ with $\mathrm{diam}(\bar{\omega}) \geq \sin(\underline{\phi}/2)$. We may write $A_z = [A_{z,1}^T \, A_{z,2}^T]^T$ where $A_{1,z}$ corresponds to the nodes in $\bar{\omega}$ and $A_{z,2}$ corresponds to the rest of the nodes in ω_z. Hence, $B_z = A_{z,1}^T A_{z,1} + A_{z,2}^T A_{z,2}$. Set $B_{z,1} = A_{z,1}^T A_{z,1}$. Since $\bar{\omega}$ satisfies both the line and the angle conditions, both B_z and $B_{z,1}$ are positive definite. Moreover, $\sigma_6(B_z) \geq \sigma_6(B_{z,1})$. Hence,

$$\sigma_6(A_z) = \sqrt{\sigma_6(B_z)} \geq \sqrt{\sigma_6(B_{z,1})} = \sigma_6(A_{z,1}).$$

Using the results established for internal nodes, $\sigma_6(A_z) \geq \tilde{C}_1 > 0$ for all $z \in \partial\Omega$.

Next, we prove the second inequality about $\sigma_n(M_z)$. Again, let $z \in \mathcal{N}_h$ and let $\mathcal{K}_z$ be its corresponding patch. By the fourth condition, non of the mesh triangles in $\mathcal{K}_z$ is degenerate. Since $\sigma_6(A_z) \geq C_1 > 0$, B_z is invertible. Hence, and by Lemma 3.1, $\mathrm{Rank}\, M_z = n$. Since the rank of a matrix can be viewed as the number of its non zero singular values, $\sigma_n(M_z) > 0$. Using this fact and an argument similar to the one used to establish $\sigma_6(A_z) \geq C_1 > 0$, one can show that $\sigma_n(M_z) \geq C_3 > 0$. □

4 Superconvergence Property of the PPR-Recovered Gradient

The following theorem establishes the superconvergence property for the PPR-recovered gradient.

Theorem 4.1. *Let $\mathcal{T}_h$ be a triangulation of Ω that satisfies the condition (α, σ) and the assumptions in Theorem 3.3. If $u \in W^3_\infty(\Omega)$, then*

$$\|\nabla u - \mathrm{G^h} u_h\|_{L^2(\Omega)} \leq Ch^{1+\rho}\|u\|_{3,\infty,\Omega},$$

where $\rho = \min(\alpha, \frac{1}{2}, \frac{\sigma}{2})$.

Proof. Since

$$\nabla u - \mathrm{G^h} u_h = (\nabla u - \mathrm{G^h}(I_h u)) + (\mathrm{G^h}(I_h u - u_h)), \tag{4.1}$$

estimating $(\nabla u - \mathrm{G^h}(I_h u))$ and $\mathrm{G^h}(I_h u - u_h)$ establishes the proof. To estimate $(\nabla u - \mathrm{G^h}(I_h u))$, recall that $\mathrm{G^h}$ preserves polynomials in $P_2(\Omega)$. Hence, and as was shown in [16],

$$\|\nabla u - \mathrm{G^h}(I_h u)\|_{L^\infty(\Omega)} \leq Ch^2|u|_{3,\infty,\Omega}. \tag{4.2}$$

Therefore,

$$\|\nabla u - \mathrm{G^h}(I_h u)\|_{L^2(\Omega)} \leq Ch^2\sqrt{|\Omega|}\|u\|_{3,\infty,\Omega}. \tag{4.3}$$

To estimate $\mathrm{G^h}(I_h u - u_h)$, Theorems 3.3 and 3.2 imply the boundedness of $\mathrm{G^h}$. Thus,

$$\|\,\mathrm{G^h}(I_h u - u_h)\|_{L^2(T)} < C_1\|\nabla(I_h u - u_h)\|_{L^2(\omega_T)} \text{ for all } T \in \mathcal{T}_h. \tag{4.4}$$

Consequently,

$$\begin{aligned} \|\,\mathrm{G^h}(I_h u - u_h)\|^2_{L^2(\Omega)} &= \sum_{T\in\mathcal{T}_h} \|\,\mathrm{G^h}(I_h u - u_h)\|^2_{L^2(T)} \\ &\leq \sum_{T\in\mathcal{T}_h} C_1^2\|\nabla(I_h u - u_h)\|^2_{L^2(\omega_T)} \\ &\leq C\|\nabla(I_h u - u_h)\|^2_{L^2(\Omega)}. \end{aligned} \tag{4.5}$$

Since $\mathcal{T}_h$ satisfies the condition (α, σ),

$$\|\nabla(I_h u - u_h)\|_{L^2(\Omega)} \leq C_2 h^{1+\rho}\|u\|_{3,\infty,\Omega} \tag{4.6}$$

where $\rho = \min(\alpha, \frac{1}{2}, \frac{\sigma}{2})$. Using (4.6) in (4.5), we have

$$\|\,\mathrm{G^h}(I_h u - u_h)\|_{L^2(\Omega)} \leq Ch^{1+\rho}\|u\|_{3,\infty,\Omega}. \tag{4.7}$$

Using (4.3) and (4.7) in (4.1) completes the proof. □

Remark 4.2. The conclusion of Theorem 4.1 is true if the condition(α, σ) is replaced by any other condition that guarantees superconvergence in $\nabla(I_h u - u_h)$. But, the condition(α, σ) covers a wide range of meshes used in practice.

Remark 4.3. The regularity requirement $u \in W^3_\infty(\Omega)$ in Theorem 4.1 may not be satisfied in many practical problems. However, the conclusion in Theorem 4.1 is true on any $\Omega_0 \subset\subset \Omega_1 \subset\subset \Omega$ with $u \in W^3_\infty(\Omega_1)$. Proving this result uses standard finite element interior analysis (for example, see [13]). For a complete proof, the reader is referred to Theorem 4.3 in [15].

Consider the global *a posteriori* error estimator η_h defined by

$$\eta_h = \| \mathrm{G^h} u_h - \nabla u_h \|_{L^2(\Omega)}.$$

Corollary 4.4. *If, in addition to the assumptions in Theorem 4.1,*

$$\|\nabla(u - u_h)\|_{L^2(\Omega)} \geq c(u)h, \tag{4.8}$$

then

$$\left| \frac{\eta_h}{\|\nabla(u-u_h)\|_{L^2(\Omega)}} - 1 \right| \leq Ch^\rho.$$

Proof. By Theorem 4.1, and the assumption in (4.8), we have

$$\left| \frac{\eta_h}{\|\nabla(u-u_h)\|_{L^2(\Omega)}} - 1 \right| \leq \frac{\| \mathrm{G^h} u_h - \nabla u_h \|_{L^2(\Omega)}}{\|\nabla(u-u_h)\|_{L^2(\Omega)}} \leq \frac{Ch^{1+\rho}\|u\|_{3,\infty,\Omega}}{c(u)h} = Ch^\rho. \qquad \square$$

5 Numerical Results

In this section we will go over some numerical examples that demonstrate the superconvergence property of $\mathrm{G^h}$ and the asymptotic exactness of the $\mathrm{G^h}-$based *a posteriori* error estimator. As it is known, the SPR is one of the best gradient recovery techniques. Moreover, the computer-based theory, developed by Babuška and Strouboulis [4], showed that the SPR-based *a posteriori* error estimator is the most robust one. Hence, quality of the PPR can be measured using the SPR as a reference.

As before, the gradient recovery operator associated with either the SPR or the PPR is denoted by R_h. The examples considered in this section are based on the model problem

$$-\triangle u = f \text{ in } \Omega \text{ and } u = g \text{ on } \partial\Omega.$$

In general, the quality of $R_h u_h$ deteriorates near $\partial\Omega$. Therefore, we should study the behavior of $R_h u_h$ inside Ω and near $\partial\Omega$ separately. To distinguish between the regions inside Ω and the ones adjacent to $\partial\Omega$, $\mathcal{N}_h$ is partitioned into $\mathcal{N}_{h,1} \cup \mathcal{N}_{h,2}$, where

$$\mathcal{N}_{h,1} = \{z \in \mathcal{N}_h : \mathrm{dist}(z, \partial\Omega) \geq H\}$$

for some $H > 0$. Next, $\overline{\Omega}$ is partitioned into $\Omega_1 \cup \Omega_2$, where

$$\Omega_1 = \bigcup \{T \in \mathcal{T}_h : T \text{ has all of its vertices in } \mathcal{N}_{h,1}\}.$$

Let $\mathcal{A} \subseteq \overline{\Omega}$ be the union of a set of mesh triangles in $\mathcal{T}_h$. The R_h−based *a posteriori* error estimator in $\mathcal{A}$ is

$$\eta_{h,\mathcal{A}} = \|R_h u_h - \nabla u_h\|_{L^2(\mathcal{A})}.$$

To measure the accuracy of $\eta_{h,\mathcal{A}}$, we use the effectivity index $\theta_{h,\mathcal{A}}$ defined by

$$\theta_{h,\mathcal{A}} = \frac{\eta_{h,\mathcal{A}}}{\|\nabla(u - u_h)\|_{L^2(\mathcal{A})}}.$$

It is customary to use colorful pictures to trace the accuracy of the *a posteriori* error estimator in each of the mesh triangles in $\mathcal{A}$. Instead, we will trace the mean, $\mu_{h,\mathcal{A}}$, and the standard deviation, $\sigma_{h,\mathcal{A}}$, of the effectivity indices in these triangles. If the estimator is asymptotically exact in each of the triangles in $\mathcal{A}$, then $\mu_{h,\mathcal{A}} \to 1$ and $\sigma_{h,\mathcal{A}} \to 0$ as $h \to 0$. Note that

$$\mu_{h,\mathcal{A}} = \frac{1}{N_{h,\mathcal{A}}} \sum_{T \subset \mathcal{A}} \theta_{h,T}$$

and

$$\sigma^2_{h,\mathcal{A}} = \frac{1}{N_{h,\mathcal{A}}} \sum_{T \subset \mathcal{A}} (\theta_{h,T} - \mu_{h,\mathcal{A}})^2$$

where $N_{h,\mathcal{A}}$ is the number of mesh triangles in $\mathcal{A}$.

Example 1. In this example $\Omega = (0,1)^2$, the solution is $u = \sin(\pi x)\sin(\pi y)$, and H is 1/8. For mesh generation we consider two cases.

In the first case, we start with an initial mesh generated by the Delauny triangulation with $h = 0.1$ as shown in Fig. 6(a). From this figure, it is clear that the Delauny-generated mesh satisfy the condition (α, σ) with α close to 1 and σ relatively large. Moreover, this mesh satisfies the conditions in Theorem 3.3. Hence, $\mathrm{G^h}$ is bounded, Theorem 1.3 is applicable, and the PPR-recovered gradient enjoys superconvergence. In successive iterations, the new mesh is obtained from the old one by regular refinement. The results are shown in Fig. 6(b) and Fig. 6(c), where we can note two things. First, although the PPR and the SPR have almost the same global behavior in Ω_1, the statistics shows that the PPR is slightly better when we consider the local behavior. Secondly, the global and local properties of the PPR is much better when it comes to Ω_2.

In the second case, the successive meshes are obtained by decomposing the unit square into $N \times N$ equal squares and then divide every square into two triangles such that the mesh triangles are arranged in the Chevron pattern. This is done for $N = 16, 32$, and 64. The mesh for $N = 16$ is shown in Fig. 7(a). Before we go over the results for this case, note that $\mathrm{G^h}$ is bounded and that Theorem 1.3 is not applicable as any pair of triangles sharing a vertical edge form a bigger triangle, not a parallelogram. As shown in Fig. 7(b), we can see that $\nabla(I_h u - u_h)$ has superconvergence that enables $\mathrm{G^h}$ to produce superconvergent recovered gradient as mentioned in Remark 4.2. This is not the case with the SPR as it does not preserve polynomials of order 2. Consequently, the behavior of the *a posteriori* error estimator based on the SPR is inferior to that based on the PPR as shown in Fig. 7(c). We can see that the error estimator based on the SPR is underestimating the actual error in Ω_1 and is overestimating it in Ω_2. However, the PPR error estimator is asymptotically exact in both Ω_1 and Ω_2. Moreover, the statistics in Fig. 7(c) shows that the PPR error estimator is asymptotically exact in each of the mesh triangles.

Example 2. In this example $\Omega = (-1,1)^2 \setminus [1/2,1)^2$. Using a polar coordinate system at (1/2,1/2), the solution is $u = r^{\frac{1}{3}} \sin\left(\frac{2\theta - \pi}{3}\right)$ where $\pi/2 \leq \theta \leq 2\pi$. As before, H is 1/8, and we start with an initial mesh generated with the Delauny triangulation at $h = 0.2$. Since we have singularity at the reentrant corner (1/2,1/2), we have to refine the triangles near this point in the initial mesh so that the pollution effect is minimized. So, after getting the Delauny triangulation we use regular refinement for the triangles that are within 0.1 from (1/2,1/2). This will serve as our initial mesh which is shown in Fig. 8(a). In the successive iterations, the mesh is regularly refined. The numerical results for this example are shown in Fig. 8(b) and Fig. 8(c). We should note that the mesh in this example, even after the refinement near the reentrant corner, is not as good as the one in Fig. 7(a). We can see many pairs of triangles that do not form "good" quadrilaterals, i.e., σ is relatively small. Also, because of the singularity at the reentrant corner (1/2,1/2), we expect both the PPR and the SPR to behave badly near this point. Of course, this affects the convergence rates for the recovered gradients, especially in Ω_1, but still the PPR yields some what better results, even on individual mesh triangles.

In conclusion, under mild conditions, we have shown that $\mathrm{G^h}$ can detect any superconvergence in $\nabla(I_h u - u_h)$ and reflects it in the recovered gradient. Consequently, the PPR error estimator is asymptotically exact, at least globally. The numerical examples indicate that the PPR is, at least, as good as the SPR both inside Ω and near the $\partial\Omega$.

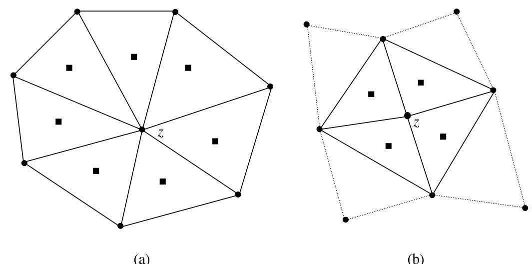

Fig. 1. Patches used in gradient recovery at an internal mesh node z. Sampling points for the SPR are marked with ■ while those needed for the PPR are marked with •

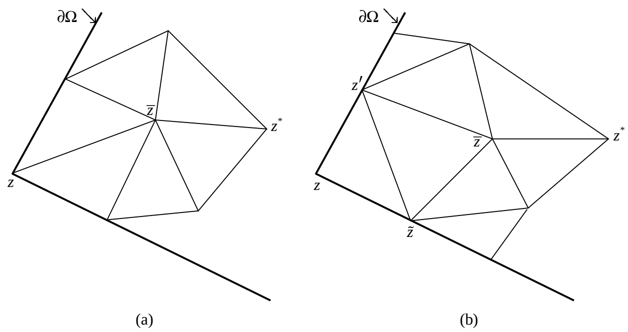

Fig. 2. Examples for patches used in the PPR at a boundary mesh node z.

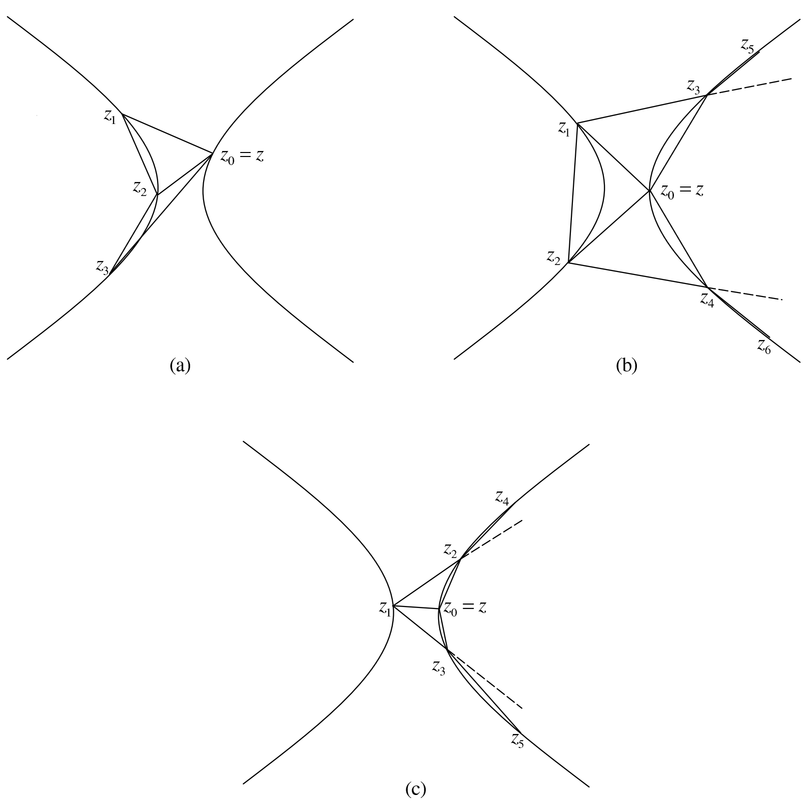

Fig. 3. Nodes in ω_z can not be distributed on two branches of a hyperbola when ω_z satisfies the angle condition.

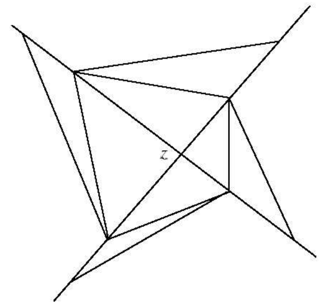

Fig. 4. An example for patch $\mathcal{K}_z$, corresponding to an internal mesh node z, that does not satisfy the line condition

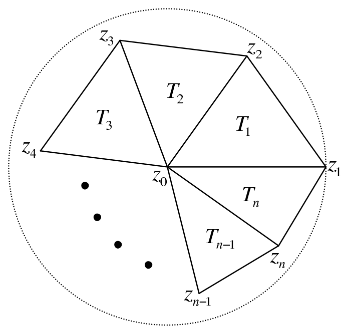

(a) $n_1 > 4$

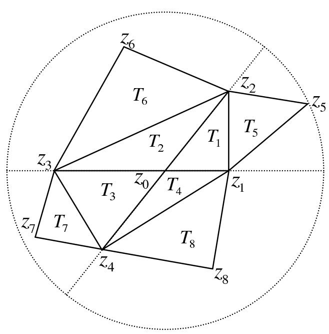

(b) $n_1 = 4$ and $n = 8$

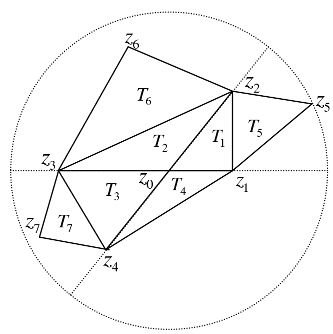

(c) $n_1 = 4$ and $n = 7$

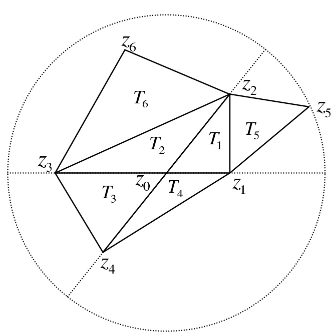

(d) $n_1 = 4$ and $n = 6$

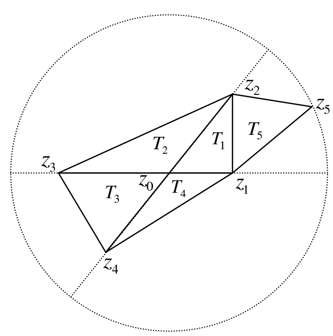

(e) $n_1 = 4$ and $n = 5$

Fig. 5. The possible patterns for a patch $\mathcal{K}_z$ corresponding to an internal mesh node z.

(a) Initial Mesh

(b) Properties of $\mathrm{R}_h u_h$

(c) Properties of θ_h

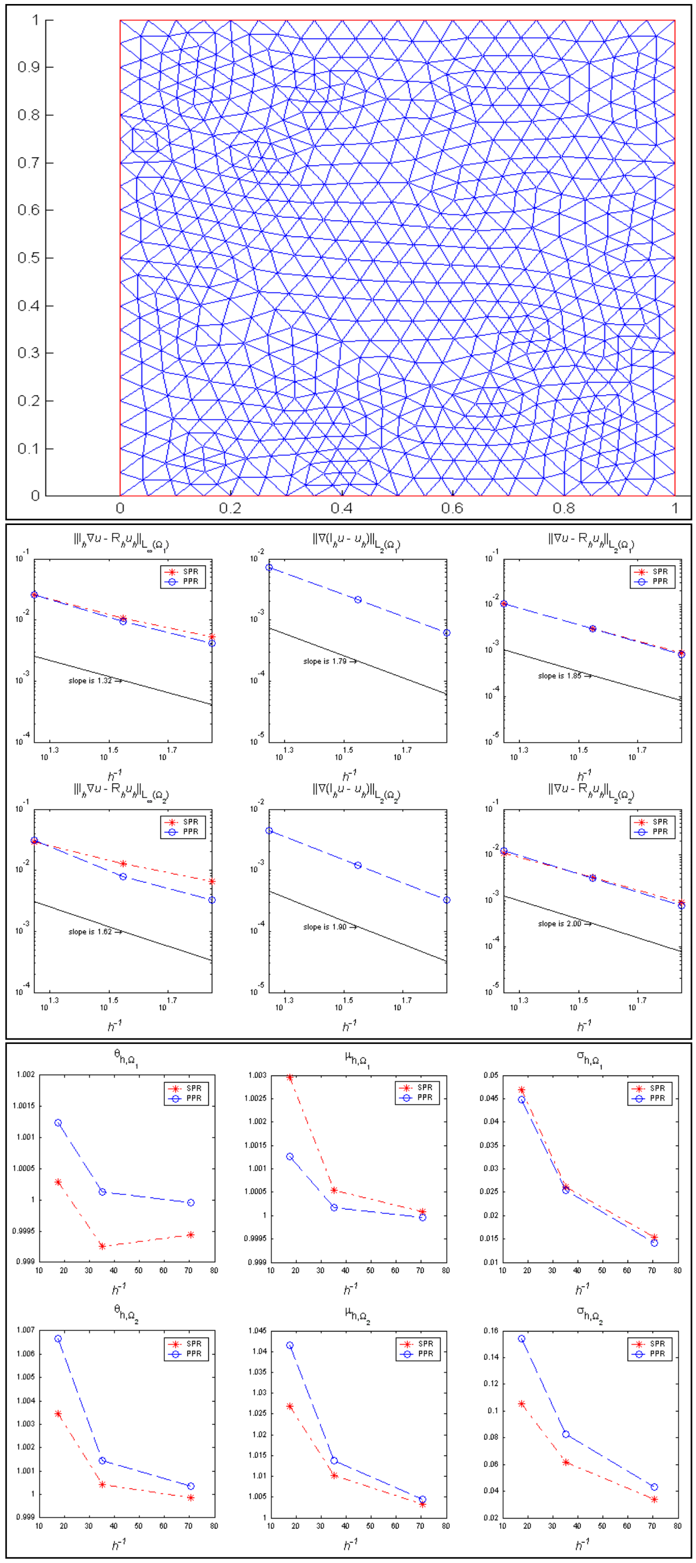

Fig. 6. Example 1 (Delauny triangulation).

(a) Initial Mesh

(b) Properties of $\mathrm{R}_h u_h$

(c) Properties of θ_h

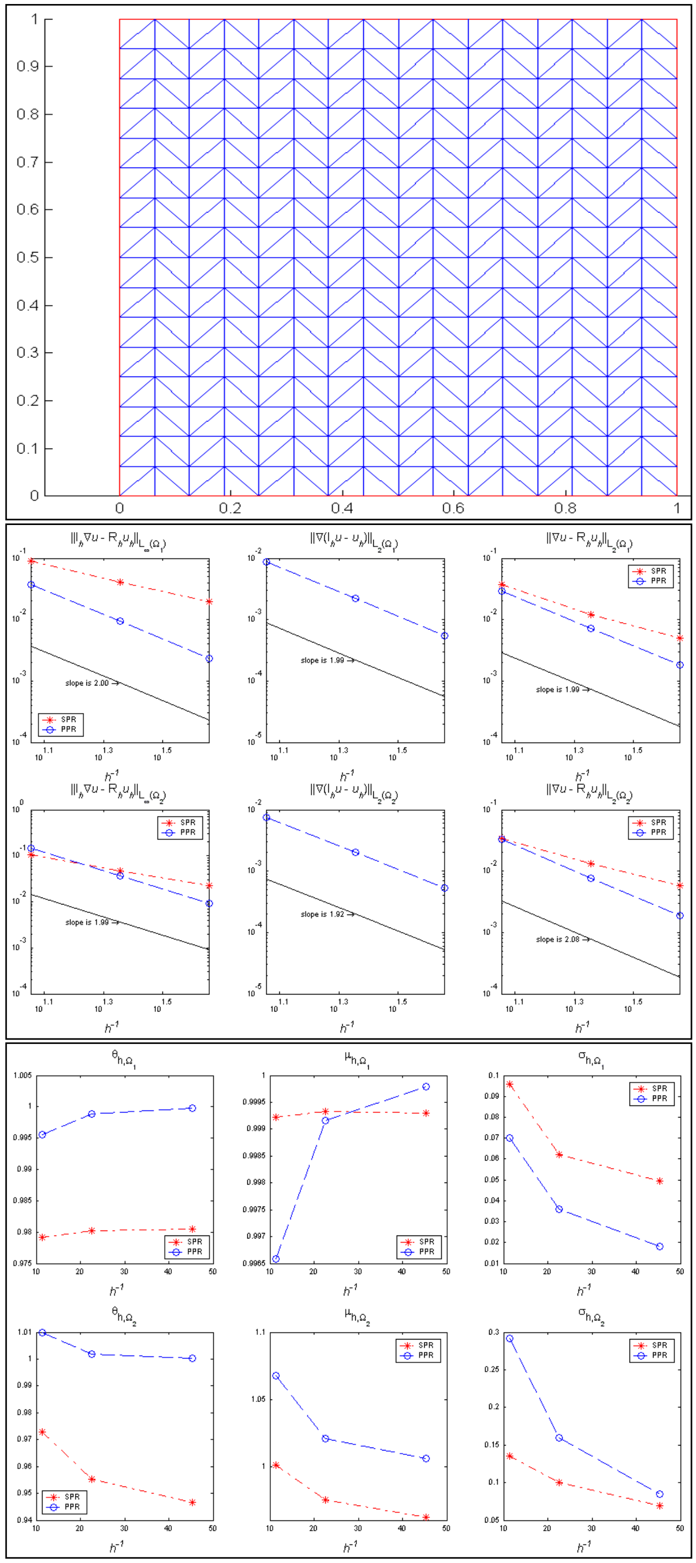

Fig. 7. Example 1 (Chevron mesh).

(a) Initial Mesh

(b) Properties of $R_h u_h$

(c) Properties of θ_h

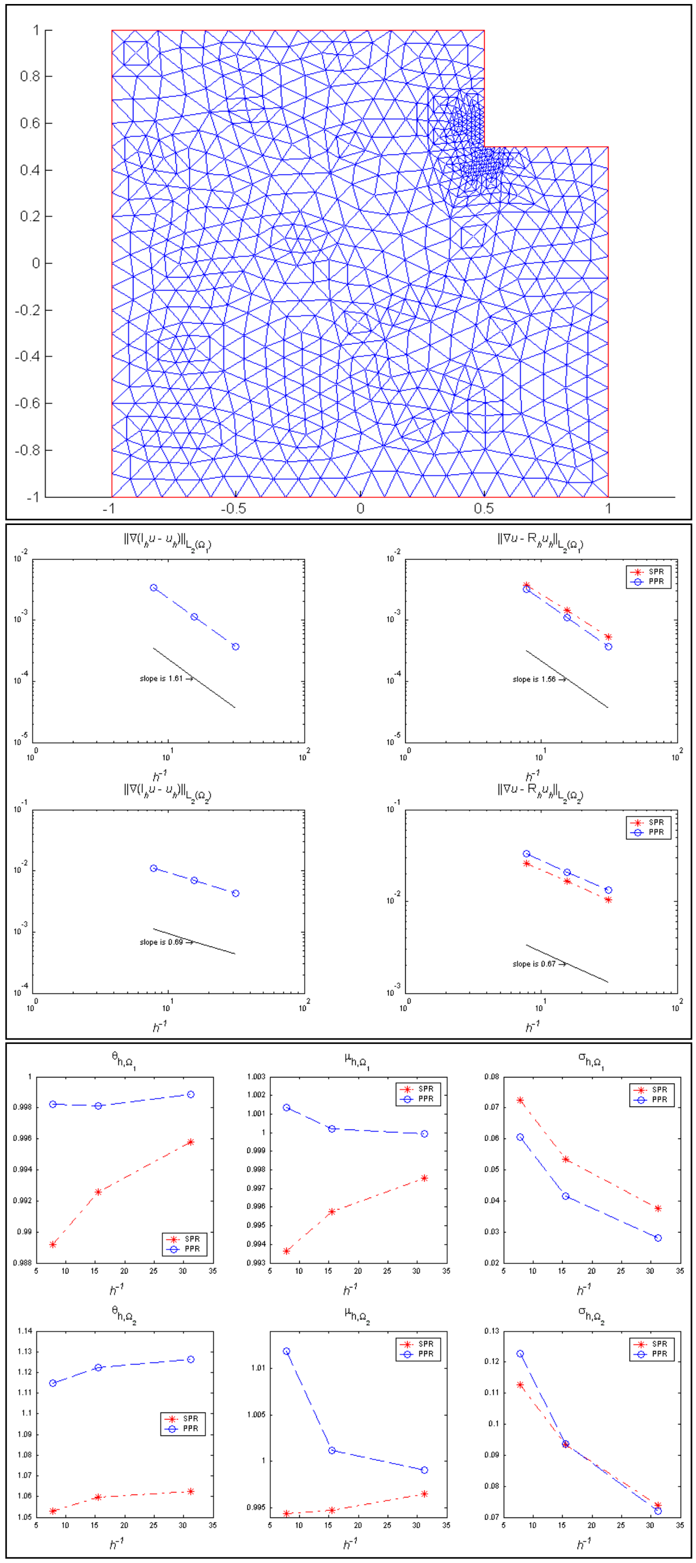

Fig. 8. Example 2.

References

[1] Ainsworth, M., Oden, J.T., *A POSERIORI ERROR ESTIMATION IN FINITE ELEMENT ANALYSIS*, Wiley Interscience, New York, 2000, pp. 73-77.

[2] Babuška, I., Aziz, A.K., *On the angle condition in the finite element method*, SIAM J. Numer. Anal., 13 (1976), pp. 214-226.

[3] Babuška, I., Rheinboldt, W.C., *A posteriori error estimates for the finite element method*, Internat. J. Numer. Methods Eng, 12 (1978), pp. 1597-1615.

[4] Babuška, I., Strouboulis, T., *THE FINITE ELEMENT METHOD AND ITS RELIABILITY*, Oxford University Press, London, 2001.

[5] Bank, R.E., *Hierarchical bases and the finite element method*, Acta Numerica, 1996, pp. 1-43.

[6] Bank, R.E., Weiser, A., *Some a posteriori error estimators for elliptic partial differential equations*, Math. Comp., 44 (1985), pp.283-301.

[7] Bank, R.E., Xu, J., *Asymptotically exact a posteriori error estimators, part I: grids with superconvergence*, (submitted for review)

[8] Blum, H., Lin, Q., Rannacher, R., *Asymptotic error expansion and richardson extrapolation for linear finite elements*, Numer. Math., 49 (1986), no. 1, pp. 11-37.

[9] Křížek, M., Neittaanmäki, p., Stenberg, R., eds, *Finite Element Methods: Superconvergence, Postprocessing, and A Posteriori Error Estimates*, Lecture Notes in Pure and Applied MAthematics Series, Vol. 196 (Marcel Dekker, New York, 1997).

[10] Li, X.D, Wiberg, N.-E., *A posteriori error estimate by element patch postprocessing, adaptive analysis in energy norm and L_2 norms*, Comput. & Structures, 53 (1994), no. 4, pp. 907-919.

[11] Lin, Qun, Xu, Jinchao, *Linear finite elements with high accuracy*, J. Comput. Math. 3 (1985), no. 2, 115–133.

[12] Verfürth, R., *A Review of A Posteriori Error Estimation and Adaptive Mesh-Refinment Techniques*, (Wiley/Teubner, Stuttgart, 1996).

[13] Wahlbin, L.B., *Superconvergence in Galerkin Finite Element Methods*, Lecture Notes in Mathematics, Vol.1605, Springer, Berlin, 1995.

[14] Wiberg, N.-E., Li, X.D, *Superconvergent patch recovery of finite element solution and a posteriori error L_2 norm estimate*, Comm. Numer. Methods Eng., 10 (1994), no. 4, pp. 313-320.

[15] Xu, J., Zhang, Z. , *Analysis of recovery type a posteriori error estimators for mildly structured grids*, Mathematics of Computations, 2003, accepted.

[16] Zhang, Z., Naga, A., *A meshless gradient recovery method, part I: superconvergence property*, Research Report #2 (2002), Department of Mathematics, Wayne State University.

[17] Zienkiewicz, O.C., Zhu, J.Z., *A simple error estimator and adaptive procedure for practical engineering analysis*, Internat. J. Numer. Methods Eng, 24 (1987), pp. 337-357.

[18] Zienkiewicz, O.C., Zhu, J.Z., *The superconvergence patch recovery and a posteriori error estimates, part I: the recovery technique*, Internat. J. Numer. Methods Eng, 33 (1992), pp. 1331-1364.

[19] Zienkiewicz, O.C., Zhu, J.Z., *The superconvergence patch recovery and a posteriori error estimates, part II: error estimates and adaptivity*, Internat. J. Numer. Methods Eng, 33 (1992), 1365-1382.